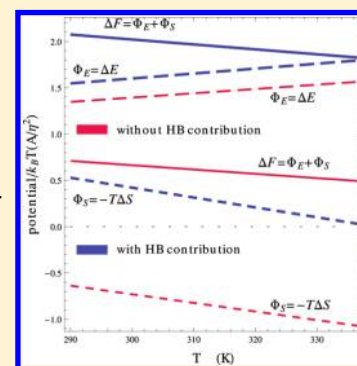


Effect of Water–Water Hydrogen Bonding on the Hydrophobic Hydration of Large-Scale Particles and Its Temperature Dependence

Y. S. Djikaev* and E. Ruckenstein†

Department of Chemical & Biological Engineering, SUNY at Buffalo, Buffalo, New York 14260, United States

ABSTRACT: We present a theoretical model for the effect of water hydrogen bonding on the thermodynamics of hydrophobic hydration. The model is based on a combination of the classical density functional theory with the recently developed probabilistic approach to water hydrogen bonding near a hydrophobic surface. This combination allows one to determine the distribution of water molecules in the vicinity of a hydrophobic particle and calculate the thermodynamic quantities of hydrophobic hydration as well as their temperature dependence. The probabilistic approach allows one to implement the effect of the hydrogen bonding ability of water molecules on their interaction with the hydrophobic surface into the formalism of density functional theory. This effect arises because the number and energy of hydrogen bonds that a water molecule forms near a hydrophobic surface differ from their bulk values. Such alteration gives rise to a hydrogen bond contribution to the external potential field whereto a water molecule is subjected in that vicinity. This contribution is shown to play a dominant role in the interaction of a water molecule with the surface. Our approach predicts that in the temperature range from 293 to 333 K: (a) the free energy of hydration of a planar hydrophobic surface in a model liquid water increases with increasing temperature (although its ratio to the temperature decreases); (b) the hydration process is unfavorable both enthalpically and entropically; (c) the entropic contribution to the hydration free energy is much smaller than the enthalpic one and decreases with increasing temperature, potentially becoming negative. The latter is indirectly supported by the experimental observation that under some conditions the hydration of a molecular hydrophobe is entropically favorable as well as by the molecular dynamics simulations predicting positive hydration entropy for sufficiently large hydrophobes.



1. INTRODUCTION

Particles exhibiting resistance to being either wetted by liquid water (case of meso/macroscopic ones) or dissolved therein (case of molecules) are generally referred to as hydrophobic solutes. The transfer of a hydrophobic solute into liquid water is accompanied by an increase in the free energy of the system, which results from the structural modifications of liquid water around the solute. This phenomenon is referred to as hydrophobic hydration. When two solute particles are close enough to each other, the total volume of water thus affected by both particles is smaller than when they are far apart, and this gives rise to an effective, solvent-mediated (often referred to as hydrophobic) attraction between particles.

It is believed that hydrogen bonding between neighboring water molecules^{1–3} constitutes a key element of hydrophobic effects^{4–7} (hydration and attraction) which, in turn, play a crucial role in many physical, chemical, and biological phenomena.^{7–11} The development of predictive models capable of estimating the temperature and pressure dependence of hydrophobic phenomena is therefore quite important.

In attempts to understand hydrophobic effects at a fundamental level and to develop a generally satisfactory theory of hydrophobicity,^{12,13} various mechanisms have been suggested^{4–7,14–21} (mostly involving the hydrogen bonding ability of water molecules). Despite many remaining controversies, the dependence of hydrophobic phenomena on the length scales of hydrophobic particles involved appears to be out of contention.^{22–25}

Small hydrophobic molecules (whereof the linear size is comparable to that of a water molecule) can fit into the water hydrogen-bond network without destroying any bonds.¹⁵ On one hand, this results in a negligible enthalpy of hydration; on the other hand, the presence of the solute is thought to constrain some degrees of freedom of the neighboring water molecules and hence to give rise to a negative entropy of hydration proportional to the solute excluded volume. Consequently, the hydration free energy is positive and increases with temperature and solute excluded volume.

Since the hydration of small hydrophobic molecules is entropically “driven”, so is their solvent-mediated interaction.^{12,13} At small enough separations, the two hydrophobic molecules affect fewer solvent molecules than when they are far apart. Therefore, bringing two hydrophobic molecules sufficiently close to each other should result in a positive change of the entropy and should thereby lower the free energy of the solution (small enthalpy changes are neglected).

Although attractive owing to its simplicity, such a mechanism of small-scale hydrophobicity appears to be somewhat inaccurate.^{12,13} Simulations^{26,27} and theory¹⁶ showed that two inert gas molecules (such as argon) would not be driven together to form a dimer; a solvent-separated pair would be a more likely

Received: October 25, 2011

Revised: January 17, 2012

Published: January 20, 2012

state than a contact pair. This leads to the surprising suggestion that the hydration of small hydrophobic molecules is actually entropically favorable (the entropy of the system increases), which contradicts conventional wisdom.

The hydration of large hydrophobic particles is believed to occur via a different mechanism.^{12,13,27–29} When inserted into liquid water, such a particle breaks some hydrogen bonds in its immediate vicinity. This results in a large positive enthalpy of hydration and hence in a free energy change proportional to the solute surface area (as opposed to being proportional to the solute volume for small hydrophobes).

Thus, in contrast to entropically driven small-scale hydrophobicity, the hydration of large hydrophobic particles is expected to be enthalpically driven, and so is their hydrophobic interaction. Fewer water hydrogen bonds have to be broken when two large hydrophobes are “in contact” than when they are far from each other, so there is a negative enthalpy change when such particles approach each other from larger separations. The free energy change (dominated by the enthalpy change) will be hence negative and will constitute a thermodynamic driving force for their attraction.

Among theoretical means for studying hydrophobic phenomena (as well as many others including phase transitions and phase equilibria), the methods of density functional theory^{30,31} (DFT) have been particularly efficient. The DFT formalism has been widely used for studying the density profiles and thermodynamic properties of fluids near rigid surfaces of various sizes, shapes, and nature.^{32,33}

In DFT the interaction of fluid molecules with a foreign surface is usually treated in the mean-field approximation: every fluid molecule is considered to be subjected to an external potential that arises due to its pairwise interactions with the molecules of the impenetrable substrate. This external potential gives rise to a specific contribution to the free energy functional. The minimization of the free energy functional with respect to the number density of fluid molecules (as a function of the spatial coordinate \mathbf{r}) provides their equilibrium spatial distribution. However, the effect of the impenetrable surface on the ability of fluid (water) molecules to form hydrogen bonds near the surface had been ignored so far in the conventional DFT formalism.

In the present work (that can be considered as a sequel of our recently published paper³⁴), we attempt to fill in this gap and clarify some issues concerning the hydration of large hydrophobic particles by combining the density functional theory with the recently developed probabilistic approach^{35,36} to hydrogen bonding between water molecules in the vicinity of a foreign surface. This approach provides an analytic expression for the average number of hydrogen bonds that a water molecule can form as a function of its distance to the surface. Knowing this expression, one can implement the effect of the hydrogen bonding of water molecules on their interaction with the hydrophobic surface into DFT, which is then employed to determine the distribution of water molecules near a macroscopic hydrophobic particle and to calculate the thermodynamic quantities of hydrophobic hydration and their temperature dependence.

2. OUTLINE OF A PROBABILISTIC APPROACH TO WATER–WATER HYDROGEN BONDING NEAR A HYDROPHOBIC SURFACE

Let us first briefly describe the probabilistic hydrogen bond (PHB) model^{35,36} for the hydrogen bonding ability of water

molecules. It considers a water molecule, whereof the location is determined by its center, to have four hydrogen-bonding (hb) arms (each capable of forming a single hydrogen bond) of rigid and symmetric (tetrahedral) configuration with the interarm angles $\alpha = 109.47^\circ$. Each hb-arm can adopt a continuum of orientations. For a water molecule to form a hydrogen bond with another molecule, it is necessary that the tip of any of its hb-arms coincide with the second molecule. The length of an hb-arm thus equals the length η of a hydrogen bond.

The hydrogen bond length η is assumed to be independent of whether the molecules are in the bulk or near a hydrophobic surface. The characteristic length $\tilde{\eta}$ of pairwise interactions between water and molecules constituting the substrate (flat and large enough to neglect edge effects, with its location determined by the loci of the centers of its outermost, surface molecules) plays a simple role in the hydrogen bond contribution to hydration or hydrophobic interaction.^{35,36} It ($\tilde{\eta}$) only determines the reference point for measuring the distance between water molecule and substrate, so it will be set equal to η .

Consider a “boundary” water molecule (BWM) in the vicinity of a hydrophobic substrate S (immersed in liquid water) at a distance x . Such a molecule forms a smaller number of hydrogen bonds (hereafter referred to as “boundary hydrogen bonds”) than in bulk water because the hydrophobic surface restricts the configurational space available to other water molecules that are necessary for a BWM to form hydrogen bonds. The actual number of hydrogen bonds that a particular BWM can form depends on both its location and its orientation. The PHB model allows one to obtain an analytic expression for the average number of bonds that a BWM can form as a function of its distance to the surface (“average” with respect to all possible orientations of the water molecule).^{35,36}

Note that a boundary hydrogen bond (BHB), involving at least one boundary water molecule, may be slightly altered energetically compared to the bulk one. Such alteration is still a subject of contention,³⁷ as different authors suggest opposite effects, that is, both enhancement^{18,38} and weakening^{3a} of the boundary hydrogen bonds. In the PHB approach, there is no restriction on the energy of a bulk (water–water) hydrogen bond, $\varepsilon_b < 0$, so that the approach is valid independent of whether $\varepsilon_b < \varepsilon_s$, $\varepsilon_b = \varepsilon_s$, or $\varepsilon_b > \varepsilon_s$, where $\varepsilon_s < 0$ is the energy of a BHB.

2.1. Average Number of BHBs per Water Molecule.

Let us choose a Cartesian coordinate system so that its x -axis is normal to the plate P located at $x = 0$. Denote the number of hydrogen bonds per bulk water molecule by n_b and the average number of hydrogen bonds per BWM by n_s . The latter is a function of distance x between the water molecule and the hydrophobic surface (assumed to be smooth on a molecular scale): $n_s \equiv n_s(x)$. If x is larger than 2η , the number of hydrogen bonds that the molecule can form is not affected by the presence of the surface. Therefore, $n_s(x) = n_b$ for $x \geq 2\eta$. On the other hand, the function $n_s(x)$ attains its minimum at the minimal distance between the water molecule and the plate, that is, at $x = \eta$, because at this distance the configurational space available for the neighboring water molecules (to form a bond with the selected one) is restricted (compared to the bulk water) by the plate the most. The layer of thickness η from $x = \eta$ to $x = 2\eta$ is referred to as the surface hydration layer (SHL).

The function $n_s = n_s(x)$ can be shown^{35,36} to have the form

$$n_s = k_1 b_1 + k_2 b_1^2 + k_3 b_1^3 + k_4 b_1^4 \quad (1)$$

where b_1 is the probability that one of the hb-arms (of a bulk water molecule) can form a hydrogen bond and $k_1 \equiv k_1(x)$, $k_2 \equiv k_2(x)$, $k_3 \equiv k_3(x)$, and $k_4 \equiv k_4(x)$ are coefficient-functions that can be evaluated by using geometric considerations (with their dependence on the BWM orientations being averaged). The functions $k_1(x)$, $k_2(x)$, $k_3(x)$, and $k_4(x)$ are presented in Figure 2a of ref 36. They all become equal to 1 at $x \geq 2\eta$ where eq 1 reduces to its bulk analogue, $n_b = b_1 + b_1^2 + b_1^3 + b_1^4$ (see ref 39). Since experimental data on n_b (and even its temperature dependence) are readily available, the latter equation allows one to determine the probability b_1 as its positive solution satisfying the condition $0 < b_1 < 1$.

Thus, eq 1 provides an efficient pathway to n_s as a function of x . It takes into account the constraint that some orientations of the hb-arms of a BWM cannot lead to the formation of hydrogen bonds because of the proximity to the hydrophobic particle. The severity of this constraint depends on the distance of the BWM to the surface, hence the x -dependence of k_1 , k_2 , k_3 , and k_4 . Equation 1 assumes that the intrinsic hydrogen-bonding ability of a BWM (i.e., the tetrahedral configuration of its hb-arms and their lengths and energies) are unaffected by its proximity to the hydrophobic surface so that the latter only restricts the configurational space available to other water molecules necessary for this BWM to form hydrogen bonds.

Figure 2b in ref 36 presents the function $n_s(x)$ for a hydrophobic flat surface immersed in water at temperature $T = 293.15$ K, which corresponds to $n_b = 3.65$, hence $b_1 = 0.963707$. As expected, the average number of hydrogen bonds per water molecule monotonically increases from its minimal value at $x = \eta$ (the closest possible distance to the plate) to its maximum bulk value n_b at $x = 2\eta$. Although the curve $n_s(x)$ itself is continuous, its slope is discontinuous at $x = 2\eta$. This “slope-discontinuity” is the consequence of the assumption that the plane $x = 2\eta$ serves as a sharp boundary such that on one side thereof ($x < 2\eta$) the hydrogen-bonding ability of water molecules is affected by the presence of the hydrophobic surface and on the other side thereof ($x > 2\eta$) it is not. Clearly, the transition from “affected” to “unaffected” molecules in real systems (liquid water in the vicinity of a hydrophobic surface) occurs smoothly over some range of x , so that not only the corresponding function $n_s(x)$ but also its first derivative $dn_s(x)/dx$ are continuous at $x = 2\eta$. The latter feature was captured in the molecular dynamics (MD) simulations⁴⁰ of the association process of two large hydrophobic plates in an extended simple point charge model (SPC/E) model water (liquid) which reported the function $n_s(x)$ to smoothly approach (although with some oscillations) its bulk value with increasing distance from a hydrophobic surface. In our PHB model the first derivative $dn_s(x)/dx$ has a finite discontinuity at $x = 2\eta$, which indicated some inaccuracy in the function $n_s(x)$ in the very close vicinity of this point. However, in this vicinity (of $x = 2\eta$) the deviation of $n_s(x)$ from n_b is very small (compared to n_b), so the inaccuracy in $n_s(x)$ can be expected to have a negligible effect on the density distribution of water molecules (see the next subsection).

2.2. Hydrogen-Bond Contribution to the Interaction of a Water Molecule with a Hydrophobic Plate. Knowing the function $n_s(x)$, one can examine the effect of water hydrogen bonding on the hydration of hydrophobic (and even composite) particles as well as on their solvent-mediated interaction. For example, let us derive an expression for $U_{\text{ext}}^{\text{hb}} \equiv U_{\text{ext}}^{\text{hb}}(x)$, the water–water hydrogen bond contribution to the total external potential field $U_{\text{ext}} \equiv U_{\text{ext}}(x)$ where to a water molecule is subjected in the vicinity of a hydrophobic surface.

The latter is needed for the application of DFT methods to the thermodynamics of hydrophobic phenomena.

The hydrogen-bond contribution $U_{\text{ext}}^{\text{hb}}$ is due (see ref 34) to the deviation of n_s from n_b and the (possible) deviation of ε_s from ε_b . It can be determined as

$$U_{\text{ext}}^{\text{hb}} \equiv U_{\text{ext}}^{\text{hb}}(x) = \varepsilon_s(x)n_s(x) - \varepsilon_b n_b \quad (\eta \leq x < \infty) \quad (2)$$

The first term on the right-hand side of this equation represents the total energy of hydrogen bonds of a water molecule at a distance x from the surface, whereas the second term is the energy of its hydrogen bonds in bulk (i.e., at $x \rightarrow \infty$). Note that the dependence of $U_{\text{ext}}^{\text{hb}}$ on x may be due not only to the function $n_s(x)$ but also to the x -dependence of the hydrogen bond energy in the vicinity of the hydrophobic surface, $\varepsilon_s \equiv \varepsilon_s(x)$. In the PHB model $n_s(x) = n_b$ for $x \geq 2\eta$, hence it is reasonable to assume that $\varepsilon_s(x) = \varepsilon_b$ for $x \geq 2\eta$ as well. Thus, $U_{\text{ext}}^{\text{hb}}(x)$ is a very short-ranged function of x , such that $U_{\text{ext}}^{\text{hb}}(x) = 0$ for $x \geq 2\eta$.

3. OUTLINE OF THE METHODS OF DENSITY FUNCTIONAL THEORY

Knowing the function $U_{\text{ext}}^{\text{hb}}(x)$, one can examine the effect of water–water hydrogen bonding on the density profile of (liquid) water molecules in the vicinity of a hydrophobic surface by using DFT.^{30–33,41,42} In this formalism, the grand thermodynamic potential Ω of a nonuniform single component fluid of volume V at a temperature T and (externally imposed) chemical potential μ (an open thermodynamic system), subjected to an external potential field U_{ext} can be represented as a functional of the number density $\rho(\mathbf{r})$ of fluid molecules

$$\Omega[\rho(\mathbf{r})] = \mathcal{F}[\rho(\mathbf{r})] + \int d\mathbf{r} U_{\text{ext}}(\mathbf{r})\rho(\mathbf{r}) - \mu \int d\mathbf{r} \rho(\mathbf{r}) \quad (3)$$

where $\mathcal{F}[\rho(\mathbf{r})]$, the intrinsic Helmholtz free energy of the system as a functional of $\rho(\mathbf{r})$, includes the contributions from fluid–fluid interactions as well as the ideal gas term. Conventionally, $\mathcal{F}[\rho(\mathbf{r})]$ is divided into two parts,

$$\mathcal{F}[\rho(\mathbf{r})] = \mathcal{F}_{\text{h}}[\rho(\mathbf{r})] + \mathcal{F}_{\text{a}}[\rho(\mathbf{r})] \quad (4)$$

where $\mathcal{F}_{\text{a}}[\rho(\mathbf{r})]$ arises from attractive forces between fluid molecules, whereas $\mathcal{F}_{\text{h}}[\rho(\mathbf{r})]$ represents the repulsive forces (and includes the ideal gas contribution as well). In the van der Waals approximation the attractive forces are treated in a mean-field fashion, while the repulsive interactions are often modeled as those of hard spheres, so that eq 4 is approximated by

$$\mathcal{F}[\rho(\mathbf{r})] = \mathcal{F}_{\text{h}}[\rho(\mathbf{r})] + \frac{1}{2} \int d\mathbf{r} d\mathbf{r}' \rho(\mathbf{r})\rho(\mathbf{r}')\phi_{\text{a}}(|\mathbf{r} - \mathbf{r}'|) \quad (5)$$

where $\mathcal{F}_{\text{h}}[\rho(\mathbf{r})]$ is the intrinsic Helmholtz free energy functional of a hard sphere fluid and $\phi_{\text{a}}(|\mathbf{r} - \mathbf{r}'|)$ is the attractive part of the interaction potential between two fluid molecules located at \mathbf{r} and \mathbf{r}' .

As the free energy functional of a three-dimensional hard-sphere fluid is not known exactly, further approximations are needed. According to the simplest one, referred to as the local density approximation (LDA),^{31–33}

$$\mathcal{F}_{\text{h}}[\rho(\mathbf{r})] = \int_V d\mathbf{r} f_{\text{h}}(\rho(\mathbf{r})) \quad (6)$$

with $f_h(\rho)$ being the Helmholtz free energy density of a hard sphere fluid of uniform density ρ . This approximation (LDA) neglects short-ranged correlations and hence cannot capture the oscillations in the density profile of a fluid near a hard wall.

The simplest ansatz for $\mathcal{F}_h[\rho(\mathbf{r})]$ that incorporates short-ranged correlations recurs^{31,41,42} to a “smoothed” or “weighted” density $\tilde{\rho}(\mathbf{r})$ which is a nonlocal functional of the actual density $\rho(\mathbf{r})$. Namely, the weighted density $\tilde{\rho}(\mathbf{r})$ at point \mathbf{r} can be regarded as a mean density obtained by averaging the actual density $\rho(\mathbf{r})$ with an appropriate “weight” function over an appropriate volume in the vicinity of \mathbf{r} . This nonlocal approximation for the intrinsic free energy functional of hard sphere fluid $\mathcal{F}_h[\rho(\mathbf{r})]$ is more accurate than LDA and is often referred to as a weighted density approximation (WDA).^{31,41,42} A key requirement of WDA is that the weight function and averaging volume should ensure that $\tilde{\rho}(\mathbf{r})$ be sufficiently smooth so that $\mathcal{F}_h[\rho(\mathbf{r})]$ can be calculated in a form formally reminiscent of local density approximation. Namely, in the framework of WDA, the intrinsic Helmholtz free energy functional of hard sphere fluid is represented in the form

$$\mathcal{F}_h[\rho(\mathbf{r})] = \int d\mathbf{r} f_i(\rho(\mathbf{r})) + \int d\mathbf{r} \rho(\mathbf{r}) \Delta\psi_h(\tilde{\rho}(\mathbf{r})) \quad (7)$$

where

$$f_i(\rho) = k_B T \rho (\ln(\Lambda^3 \rho) - 1)$$

(with $\Lambda = (h^2/2\pi m k_B T)^{1/2}$ being the thermal de Broglie wavelength of a model molecule of mass m , and h and k_B being Planck's and Boltzmann's constants, respectively) is the free energy density of an ideal gas of density ρ and

$$\Delta\psi_h(\rho) = \frac{1}{\rho} [f_h(\rho) - f_i(\rho)]$$

is the configurational part of the free energy of hard sphere fluid per molecule.

The weighted density $\tilde{\rho}(\mathbf{r})$ is determined in terms of $\rho(\mathbf{r})$ via an implicit equation

$$\tilde{\rho}(\mathbf{r}) = \int d\mathbf{r}' \rho(\mathbf{r}') w(|\mathbf{r}' - \mathbf{r}|; \tilde{\rho}(\mathbf{r})) \quad (8)$$

where $w(|\mathbf{r}' - \mathbf{r}|; \tilde{\rho}(\mathbf{r}))$ is the weight function. Although in more sophisticated versions^{31,41} of WDA $w(|\mathbf{r}' - \mathbf{r}|; \tilde{\rho}(\mathbf{r}))$ depends on $\tilde{\rho}(\mathbf{r})$, we will hereafter adopt its simpler version wherein the weight function is independent^{31,41} of $\tilde{\rho}(\mathbf{r})$ (see Section 5).

In a grand canonical ensemble (corresponding to an open thermodynamic system under constant μ , V , and T) the equilibrium density profile is obtained by minimizing the functional $\Omega[\rho(\mathbf{r})]$ with respect to $\rho(\mathbf{r})$, that is, by solving the Euler–Lagrange equation $\delta\Omega/\delta\rho = 0$ with respect to $\rho(\mathbf{r})$. The substitution of the equilibrium density profile $\rho(\mathbf{r})$ into eq 3 provides the grand thermodynamic potential Ω of the fluid.

The explicit form of the Euler–Lagrange equation significantly depends on the approximation chosen. In the framework of LDA, it is

$$\mu = \mu_h(\rho(\mathbf{r})) + \int_V d\mathbf{r}' \rho(\mathbf{r}') \phi_a(|\mathbf{r} - \mathbf{r}'|) + U_{\text{ext}}(\mathbf{r}) \quad (9)$$

where $\mu_h(\rho) \equiv df_h(\rho)/d\rho$ is the chemical potential of the uniform reference (hard sphere) fluid of density ρ , whereas in the framework of WDA it can be written as

$$\mu = k_B T \ln(\Lambda^3 \rho(\mathbf{r})) + W(\mathbf{r}; \rho(\mathbf{r})) \quad (10)$$

where

$$\begin{aligned} W(\mathbf{r}; \rho(\mathbf{r})) = & U(\mathbf{r}) + \int d\mathbf{r}' \rho(\mathbf{r}') \phi_a(|\mathbf{r} - \mathbf{r}'|) \\ & + \Delta\psi_h(\tilde{\rho}(\mathbf{r})) + \int d\mathbf{r}' \rho(\mathbf{r}') \\ & \times \Delta\psi'_h(\tilde{\rho}(\mathbf{r}')) w(|\mathbf{r}' - \mathbf{r}|) \end{aligned}$$

and $\Delta\psi'_h(\rho) \equiv d\Delta\psi_h(\rho)/d\rho$. If the constraint of constant μ (external chemical potential) is replaced by a given value of the fluid density far away from the impenetrable wall, $\rho_\infty = \rho(\mathbf{r})|_{|\mathbf{r}|=\infty}$, the Euler–Lagrange equation can be written in the form

$$\rho(\mathbf{r}) = \rho_\infty \exp \left[-\frac{1}{k_B T} (W(\mathbf{r}; \rho(\mathbf{r})) - W(\mathbf{r}; \rho_\infty)) \right] \quad (11)$$

In the canonical ensemble (corresponding to a closed thermodynamic system with constant number of molecules N , volume V , and temperature T), the chemical potential μ , which appears in eqs 3, 9, and 10, is not known in advance. Instead, it plays the role of a Lagrange multiplier corresponding to the constraint of fixed number of molecules in the system:

$$N = \int_V d\mathbf{r} \rho(\mathbf{r})$$

This equation can be used to determine the Lagrange multiplier μ , that is, the chemical potential in the system, as follows (see, e.g., ref 43).

In the case of LDA, introducing the “configurational” part of the hard sphere chemical potential as $\tilde{\mu}_h(\rho(\mathbf{r})) \equiv \mu_h(\rho(\mathbf{r})) - k_B T \ln \rho(\mathbf{r})$, one can rewrite eq 9 in the form

$$\begin{aligned} \rho(\mathbf{r}) = \exp \left\{ \frac{1}{k_B T} [\mu - U_{\text{ext}}(\mathbf{r}) - \tilde{\mu}(\rho(\mathbf{r}')) - \int d\mathbf{r}' \rho(\mathbf{r}') \right. \\ \left. \times \phi_{\text{at}}(|\mathbf{r} - \mathbf{r}'|)] \right\} \end{aligned}$$

Integrating this equation over the volume of the system and using the constraint on N , one obtains

$$\begin{aligned} \mu = k_B T \ln N - k_B T \times \ln \left(\int d\mathbf{r} \exp \left\{ \frac{1}{k_B T} [-U_{\text{ext}}(\mathbf{r}) \right. \right. \\ \left. \left. - \tilde{\mu}(\rho(\mathbf{r}')) - \int d\mathbf{r}' \rho(\mathbf{r}') \phi_a(|\mathbf{r} - \mathbf{r}'|)] \right\} \right) \end{aligned}$$

where the substitution into eq 9 yields the Euler–Lagrange equation for the density profile in the canonical ensemble:

$$\begin{aligned} \mu_h(\rho(\mathbf{r})) = & k_B T \ln N - k_B T \\ & \times \ln \left(\int d\mathbf{r} \exp \left\{ \frac{1}{k_B T} [-U_{\text{ext}}(\mathbf{r}) - \tilde{\mu}(\rho(\mathbf{r}')) \right. \right. \\ & \left. \left. - \int d\mathbf{r}' \rho(\mathbf{r}') \phi_a(|\mathbf{r} - \mathbf{r}'|)] \right\} \right) - U_{\text{ext}}(\mathbf{r}) \\ & - \int d\mathbf{r}' \rho(\mathbf{r}') \phi_a(|\mathbf{r} - \mathbf{r}'|) \end{aligned} \quad (12)$$

In the case of WDA, similar manipulations allow one to obtain the expression

$$\rho(\mathbf{r}) = N \frac{\exp[-W(\mathbf{r}; \rho(\mathbf{r}))/k_B T]}{\int d\mathbf{r} \exp[-W(\mathbf{r}; \rho(\mathbf{r}))/k_B T]} \quad (13)$$

This expression has the familiar form of a “generic” one-particle distribution function in classical statistical mechanics.⁴⁴

The Helmholtz free energy F of the canonical ensemble can then be obtained by substituting the solution of eq 6 into the corresponding functional of $\rho(\mathbf{r})$,

$$F[\rho(\mathbf{r})] = \mathcal{F}[\rho(\mathbf{r})] + \int d\mathbf{r} U_{\text{ext}}(\mathbf{r})\rho(\mathbf{r}) \quad (14)$$

with $\mathcal{F}[\rho(\mathbf{r})]$ provided either by eqs 5 and 6 (for LDA) or eqs 5 and 7 (for WDA).

As already mentioned, the function $U_{\text{ext}}(\mathbf{r})$ in the above equations had been conventionally meant to represent the external potential exerted by all of the molecules constituting the hydrophobic substrate on a fluid molecule. Various models for the external potential were designed to take into account pairwise interactions of a fluid molecule with the molecules of the substrate^{32,33} as well as the effect of the latter on the pairwise interactions between fluid molecules themselves.⁴⁵ The contribution of these (pairwise) effects into U_{ext} will be denoted by $U_{\text{ext}}^{\text{pw}}$ to distinguish it from the hydrogen bond contribution, $U_{\text{ext}}^{\text{hb}}$. Thus, the overall external potential where a water molecule is subjected near a hydrophobic surface can be represented as

$$U_{\text{ext}}(\mathbf{r}) = U_{\text{ext}}^{\text{pw}}(\mathbf{r}) + U_{\text{ext}}^{\text{hb}}(\mathbf{r}) \quad (15)$$

In the particular case of (fluid) water near a flat hydrophobic surface, one can use the planar symmetry of the system and choose the Cartesian coordinates so that the surface is located in the y - z plane at $x = 0$ with the molecules of the fluid occupying the “half-space” $x > 0$. The equilibrium density profile obtained from eq 9, 10, or 11 is then a function of a single variable x , that is, $\rho(\mathbf{r}) = \rho(x)$.

4. FREE ENERGY OF HYDRATION AND ITS TEMPERATURE DEPENDENCE

In a canonical ensemble, the free energy ΔF of hydration of a hydrophobic particle can be determined as the difference

$$\Delta F = F - F_0 \quad (16)$$

where F and F_0 are the Helmholtz free energies of the system (liquid water) with and without a hydrophobic particle therein, respectively. Likewise, the free energy of hydrophobic hydration in a grand canonical ensemble can be determined as

$$\Delta\Omega = \Omega - \Omega_0 \quad (17)$$

where Ω and Ω_0 are the values of the grand thermodynamic potential of the system (liquid water) with and without a hydrophobic particle therein, respectively.

Knowing the free energy of hydrophobic hydration, one can find Φ_S and Φ_E , the entropic and energetic contributions to ΔF , as

$$\begin{aligned} \Phi_S &\equiv -T\Delta S = T(\partial\Delta F/\partial T)_{V,N} \\ \Phi_E &\equiv \Delta E = (\partial(\Delta F/T)/\partial(1/T))_{V,N} \end{aligned} \quad (18)$$

respectively, such that $\Delta F = \Phi_E + \Phi_S$ (in eq 18 the subscripts of the partial derivatives indicate the thermodynamic variables

held constant upon taking the derivatives). Clearly, for the decomposition of ΔF into energetic and entropic components it is necessary to know its temperature dependence. (Note that a similar decomposition can be carried out for $\Delta\Omega$.)

In the combined PHB/DFT-based model presented above, the temperature dependence of ΔF contains a contribution from the temperature dependence of $U_{\text{ext}}^{\text{hb}}$, the hydrogen-bond contribution to the overall external field exerted by the hydrophobic surface on water molecules in its vicinity. As is clear from eq 2, the dependence of $U_{\text{ext}}^{\text{hb}}$ on T is due to the temperature dependence of four quantities: n_s , n_b , ε_s , and ε_b . The functions $\varepsilon_b \equiv \varepsilon_b(T)$ and $n_b \equiv n_b(T)$ are either readily available or can be constructed on the basis of available data. On the other hand, n_s is unambiguously related to n_b ; hence its dependence on T can be considered to be known as well. Finally, the dependence of ε_s on T is not known (not to mention some ambiguities in the definition of a hydrogen bond and its parameters^{1,46}), but one can expect that the energy of a hydrogen bond depends on temperature in such a way that the ratio $\varepsilon_s(T)/\varepsilon_b(T)$ varies relatively weakly with T , so that one can neglect the first- and higher-order derivative terms in the Taylor series expansion of $\varepsilon_s(T)/\varepsilon_b(T)$ with respect to the deviation of T from some middle temperature T_0 (say, room temperature, 293.15 K). Therefore, for the sake of simplicity, one can assume the ratio $\varepsilon_s(T)/\varepsilon_b(T)$ to be independent of T . One can thus consider $U_{\text{ext}}^{\text{hb}}$ to be a known function of not only x but also T , $U_{\text{ext}}^{\text{hb}} = U_{\text{ext}}^{\text{hb}}(x, T)$. This allows one to numerically determine the temperature dependence of ΔF and to subsequently use interpolation procedure to find an accurate analytical fit which then can be used in eq 18.

5. NUMERICAL EVALUATIONS

To illustrate the above model with numerical calculations, we have considered the hydration of a flat, macroscopic hydrophobic surface in a model liquid water. The pairwise interactions between two water molecules 1 and 2 were modeled with the Lennard–Jones (LJ) potential,

$$\phi_{\text{ww}} = 4\varepsilon_{\text{ww}} \left[\left(\frac{d}{r_{12}} \right)^{12} - \left(\frac{d}{r_{12}} \right)^6 \right]$$

where r_{12} is the distance between molecules 1 and 2, ε_{ww} is the energy parameter, and d is the diameter of a model molecule. The parameter ε_{ww} was adjusted to be 3.79×10^{-14} , which differs from its values used in the computer simulations (Monte Carlo or molecular dynamics) of various water models, in which ε_{ww} ranges^{3b} from 5.31×10^{-15} erg (ST2 model) to 1.47×10^{-14} erg (SWM4-NDP model) to 2.54×10^{-13} erg (SSD model). Such a modification was needed to ensure that the phase diagram of model water more or less resembles that of real water. In the DFT formalism this can be achieved only by adjusting the single intermolecular potential describing water–water interactions, whereas in computer simulations water–water interactions are usually described by the combination of LJ and electrostatic potentials; hence the difference in the energy parameters of the respective LJ potentials. The parameter d of the LJ potential also has different values in different water models^{3b} in the range from 3.02 Å (SSD model) to 3.18 Å (SWM4-NDP model). On the other hand, the length η of the hydrogen bond (i.e., the distance between the oxygen atoms of two hydrogen-bonded water molecules) is reported^{3b}

to be about 2.98 Å. Since d (of various water models) and η are so close to each other, we assumed for our model $d \simeq \eta$.

To find the equilibrium density profile of (model) water molecules in the vicinity of the hydrophobic surface, it is necessary to solve eq 9, 10, 11, 12, or 13 using an iterative procedure whereby the density profile $\rho_i(x)$ at the i th iteration is found from the previous one, $\rho_{i-1}(x)$. Namely, in LDA the iterations are performed via the equations

$$\mu_h(\rho_i(x)) = \mu - \int_V d\mathbf{r}' \rho_{i-1}(x) \phi_{at}(|\mathbf{r} - \mathbf{r}'|) - U_{ext}(x) \quad (19)$$

and

$$\begin{aligned} \mu_h(\rho_i(x)) = k_B T \ln N - k_B T \times \ln \left(\int d\mathbf{r} \exp \left\{ \frac{1}{k_B T} [-U_{ext}(x) \right. \right. \\ \left. \left. - \bar{\mu}(\rho_{i-1}(x')) - \int d\mathbf{r}' \rho_{i-1}(x') \phi_{at}(|\mathbf{r} - \mathbf{r}'|)] \right\} \right) \\ \left. - U_{ext}(x) - \int d\mathbf{r}' \rho_{i-1}(x') \phi_{at}(|\mathbf{r} - \mathbf{r}'|) \right) \quad (20) \end{aligned}$$

(for the canonical and grand canonical ensembles, respectively) whereas in WDA the iterations are carried out via the equations

$$\begin{aligned} \mu = k_B T \ln(\Lambda^3 \rho_i(\mathbf{r})) + W(\mathbf{r}; \rho_{i-1}(\mathbf{r})) \quad \text{or} \\ \rho_i(\mathbf{r}) = \rho_\infty \exp \left[-\frac{1}{k_B T} (W(\mathbf{r}; \rho_{i-1}(\mathbf{r})) - W(\mathbf{r}; \rho_\infty)) \right] \quad (21) \end{aligned}$$

and

$$\rho_i(\mathbf{r}) = N \frac{\exp[-W(\mathbf{r}; \rho_{i-1}(\mathbf{r}))/k_B T]}{\int d\mathbf{r} \exp[-W(\mathbf{r}; \rho_{i-1}(\mathbf{r}))/k_B T]} \quad (22)$$

(for the canonical and grand canonical ensembles, respectively).

For the chemical potential $\mu_h \equiv \mu_h(\rho, T)$ of a hard sphere fluid we have adopted the well-known Carnahan–Starling approximation^{32,33,47}

$$\mu_h = k_B T \left(\ln(\Lambda^3 \rho) + \xi \frac{8 - 9\xi + 3\xi^2}{(1 - \xi)^3} \right)$$

where $\xi = (\pi d^3/6)\rho$. Since μ_h is a single-valued (monotonically increasing) function of ρ , one can extract $\rho_i(x)$ from the LHS of eq 19 or 20 and continue iterations. The configurational part $\Delta\psi_h \equiv \Delta\psi_h(\rho, T)$ of the free energy of a hard sphere fluid was also modeled in the Carnahan–Starling approximation,^{32,33,47} whereas for the weight function $w(|\mathbf{r}' - \mathbf{r}|; \bar{\rho}(\mathbf{r}))$ in eq 8 we adopted a $\bar{\rho}$ -independent version:^{31,41}

$$\begin{aligned} \Delta\psi_h = k_B T \frac{\xi(4 - 3\xi)}{(1 - \xi)^2} \\ w(r_{12}) = \frac{3}{\pi\eta^4} (\eta - r_{12}) \Theta(\eta - r_{12}) \end{aligned}$$

where $\Theta(u)$ is a unit-step function: $\Theta(u) = 1$ if $u \geq 0$ and $\Theta(u) = 0$ if $u < 0$. The attractive part ϕ_a of the pairwise water–water

interactions was modeled by using a well-known perturbation scheme:⁴⁸

$$\phi_a(r_{12}) = \begin{cases} -\varepsilon_{ww} & (r_{12} < 2^{1/6}\eta) \\ \phi_{ww} & (r_{12} > 2^{1/6}\eta) \end{cases}$$

Figure 1 presents the typical behavior of U_{ext} and its components. The thick dashed curve shows U_{ext} while the lower

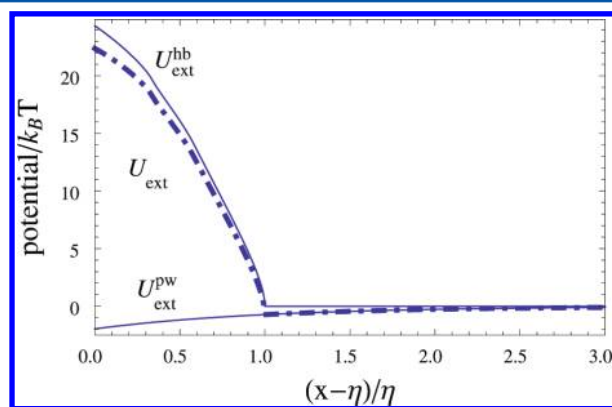


Figure 1. Typical behavior of the overall external potential U_{ext} (exerted by a hydrophobic surface on water molecules in its vicinity), shown as a thick dashed–dotted curve, and its components, U_{ext}^{pw} (lower thin solid curve) and U_{ext}^{hb} (upper thin solid curve).

and upper thin solid curves are for U_{ext}^{pw} and U_{ext}^{hb} , respectively. The function $U_{ext}^{hb}(x)$ was modeled as suggested in refs 32 and 33,

$$U_{ext}^{pw}(x) = \begin{cases} \infty & (x < \eta) \\ -\varepsilon_{sw} \exp[-\lambda_{sw}(x - \eta)] & (x > \eta) \end{cases} \quad (23)$$

where the energy parameter ε_{sw} was taken to be equal to $k_p \varepsilon_{ww}$ with $k_p = 2.1$ and the inverse length parameter λ_{sw} was set equal to $1/\eta$ (the ratio $k_p \equiv \varepsilon_{sw}/\varepsilon_{ww}$ characterizes the degree of hydrophobicity of the surface as the energy of a water molecule attraction to the surface at the distance η between them relative to $-\varepsilon_{ww}$). In $U_{ext}^{hb}(x)$ (see eq 2), the x -dependence of ε_s was approximated by a linear function increasing from its minimum value of $k_h \varepsilon_b$ at $x = \eta$ (with $k_h = 1.1$ corresponding to slightly enhanced hydrogen bonds^{18,38} for molecules closest to the hydrophobic surface) to its maximum (bulk) value ε_b for $x \geq 2\eta$. This results in $U_{ext}^{hb}(x) = \varepsilon_b n_b [(k_h - 1)(x - \eta)/\eta] n_s(x)/n_b - 1$ for $\eta \leq x < 2\eta$ and $U_{ext}^{hb}(x) = 0$ for $x \geq 2\eta$.

As clear from Figure 1, the hydrogen bonding contribution to the external potential has a repulsive character unlike the conventional pairwise contribution that has an attractive character (note also that the former dominates the latter in the most part of the range $\eta < x < 2\eta$). The repulsive character of U_{ext}^{hb} arises because the total energy of hydrogen bonds per molecule near the hydrophobic surface is smaller (in absolute value) than in the bulk, which in turn is due to $n_s(x) \leq n_b$ and $\varepsilon_s(x) \approx \varepsilon_b$ for any x .

At a given temperature, the evaluation of the free energy of hydration is simpler in a grand canonical ensemble, that is, by solving either eq 19 (for LDA) or eq 21 (for WDA), substituting the resulting equilibrium density profile in eq 3, and then calculating $\Delta\Omega$ according to eq 17. This procedure was applied

to the hydration of an infinitely large flat hydrophobic surface in the model liquid water at temperature $T = 293.15$ K.

In LDA, the chemical potential was chosen to be $\mu = -11.5989 k_B T$ corresponding to the vapor–liquid equilibrium of the model fluid. The liquid state of the bulk water was ensured by imposing the appropriate boundary condition $\rho(x) \rightarrow \rho_l$ as $x \rightarrow \infty$ onto eq 19, with ρ_l being the bulk liquid density. The densities ρ_v and ρ_l of coexisting vapor and liquid, respectively, were found by solving the pair of equations expressing the conditions of phase equilibrium at a given T ,

$$\mu(\rho, T)|_{\rho=\rho_v} = \mu(\rho, T)|_{\rho=\rho_l}$$

$$p(\rho, T)|_{\rho=\rho_v} = p(\rho, T)|_{\rho=\rho_l}$$

where $\mu(\rho, T) = \mu_h(\rho, T) - \alpha\rho$ and $p(\rho, T) = p_h(\rho, T) - (1/2)\alpha\rho^2$ with the positive constant $\alpha = -\int dr \phi_{at}(r)$.³² The pressure of a uniform hard sphere fluid $p_h = p_h(\rho, T)$ is related to the corresponding chemical potential μ_h via $\partial p_h / \partial \rho = \rho \partial \mu_h / \partial \rho$. In the Carnahan–Starling approximation^{32,33,42}

$$p_h(\rho, T) = \rho k_B T \frac{1 + \xi + \xi^2 - \xi^3}{(1 - \xi)^3}$$

For WDA, the equilibrium profile was found by solving the rightmost iterative equality in eq 21, with ρ_∞ taken as the equilibrium bulk liquid density ρ_l provided by LDA. The chemical potential, corresponding to ρ_∞ , was then calculated via eq 10 and substituted in eq 3 to obtain the grand canonical potential in WDA.

To clarify the effect of the two different contributions to $U_{\text{ext}}(x)$ on the water density distribution near the hydrophobe, the density profiles were obtained by solving eq 19 (for LDA) and eq 21 (for WDA) with the overall external potential (a) including **both** pairwise and hydrogen bond contributions (i.e., $U_{\text{ext}}(x) = U_{\text{ext}}^{\text{pw}}(x) + U_{\text{ext}}^{\text{hb}}(x)$) and (b) including **only** the pairwise component (i.e., with $U_{\text{ext}}(x) = U_{\text{ext}}^{\text{pw}}(x)$). In the former case the ratio k_h was taken to be 1.0, and in both cases various k_p were considered to mimic surfaces of various degrees of hydrophobicity. The density profiles predicted by WDA are presented in Figure 2a,b, whereas Figure 2c presents the density profiles in LDA.

In the framework of LDA, it was previously³⁴ demonstrated (see also Figure 2c) that the hydrogen-bond contribution to the external potential plays a crucial role in the formation of a thin, “strong depletion” layer (of density much lower than liquid and of thickness of a molecular diameter, in agreement with previous suggestions^{12,13}) between liquid water and hydrophobic surface even for weakly hydrophobic surfaces (with high k_p). It was also shown that, as expected, even for a relatively strong hydrophobic surface (with low k_p) the conventional contribution to the external potential (due to pairwise interactions between a water molecule and those of the substrate) cannot cause the formation of a vapor-like layer near the surface, although it does lead to a weak decrease in the vicinal fluid density compared to the bulk one.

The density profiles obtained in the framework of WDA confirm that the hydrogen-bond contribution to the external potential constitutes a cornerstone for the formation of a thin depletion layer (of thickness of a molecular diameter and of density lower than the liquid one by orders of magnitude) between liquid water and hydrophobic surface. However, as is clear from Figure 2a, density profiles in WDA become increasingly oscillating as the degree of hydrophobicity of the surface decreases,

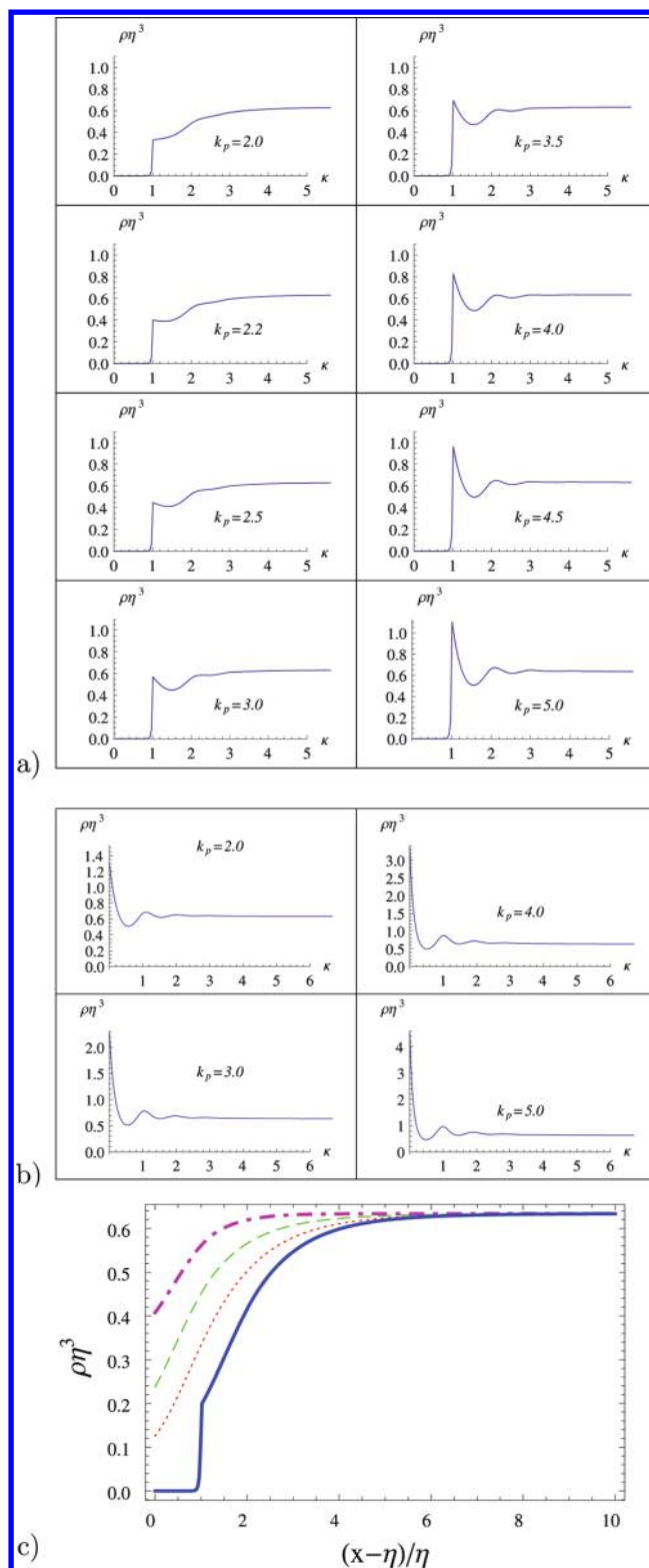


Figure 2. Density profiles of a model water fluid near an infinitely large hydrophobic surface at $T = 293.15$ K shown as $\rho(X)\eta^3$ vs $\kappa \equiv (x - \eta)/\eta$. (a) The results of WDA with $U_{\text{ext}}(x) = U_{\text{ext}}^{\text{pw}}(x) + U_{\text{ext}}^{\text{hb}}(x)$ for various k_p (indicated in each panel) and $k_h = 1.0$. (b) The results of WDA with $U_{\text{ext}}(x) = U_{\text{ext}}^{\text{pw}}(x)$ for various k_p (indicated in each panel). (c) The results of LDA with the solid curve representing the case $U_{\text{ext}}(x) = U_{\text{ext}}^{\text{pw}}(x) + U_{\text{ext}}^{\text{hb}}(x)$ for $k_p = 2.1$ and the dashed–dotted, dashed, and dotted curves representing the case $U_{\text{ext}}(x) = U_{\text{ext}}^{\text{pw}}(x)$ for three different values of k_p (2.1, 1.0, and 0.5, respectively).

that is, as k_p increases (similar dependence of water density profiles near a flat hydrophobic surface on the strength of water-surface attraction was recently reported in ref 49). This effect cannot be captured by LDA which is intrinsically unable to describe fluid density oscillations near a hydrophobic surface. Still, one can notice that, when the hydrogen-bond contribution to the external potential is taken into account (Figure 2a,c), even in WDA the fluid density oscillations are virtually nonexistent near a strongly hydrophobic surface (with $k_p \lesssim 2.2$); in both LDA and WDA the shapes of the density profiles for such surfaces are qualitatively similar, although quantitatively the differences between WDA and LDA profiles do exist. The situation is quite different when the hydrogen-bond contribution is not included into the external potential (Figure 2b,c): the density profiles in WDA exhibit strong oscillations (starting with a very high density near the surface), while in LDA the fluid density monotonically increases from its low values (although not as low as in a vapor) near the surface to its bulk liquid values far away from the surface.

Some results on the thermodynamics of hydration are presented in Figures 3–5. Note that all of the potentials in these figures are expressed in units of $k_B T$ per “dimensionless unit area”; namely, the dimensionless values shown in Figures 3–5 are obtained by dividing the corresponding potentials by $k_B T$ and by $A/\eta^2 \equiv A/\eta^2$, where A is the area of the hydrophobic surface which is being hydrated. The lines in Figures 3–5 represent the least mean squares (LMS) fits of the corresponding sets of calculated data shown as points.

Figure 3a presents the grand canonical free energy of hydrophobic hydration $\Delta\Omega$ (expressed in units of $k_B T$ per dimensionless unit area as explained above), as a function of the energetic alteration ratio k_h of hydrogen bonds (in the SHL compared to the bulk), at a constant ratio k_p (characterizing the degree of hydrophobicity of the surface). Due to the model character of the hydrophobic surface, we considered several values of k_p . Each line in Figure 3a corresponds to a constant k_p ; solid lines correspond to WDA (with $k_p = 2.0, 2.2, 2.3$, and 2.5 from top to bottom), whereas the dashed lines are the predictions of LDA (with $k_p = 2.0, 2.1, 2.2$, and 2.3 from top to bottom). As is clear, the hydrophobic hydration is hardly sensitive to the hydrogen bond energy alteration ratio, k_h , but is quite sensitive to the degree of hydrophobicity of the surface, k_p . The latter effect is also demonstrated in Figure 3b, where the dependence of $\Delta\Omega$ on k_p is shown for the case where **only** the pairwise component was included in the external potential, that is, $U_{\text{ext}}(x) = U_{\text{ext}}^{\text{pw}}(x)$. Again, the solid line is for WDA, whereas the dashed one is for LDA. Both parts a and b of Figure 3 clearly demonstrate that the more accurate WDA predicts consistently lower values for the free energy of hydration than LDA, but the difference between the two decreases with increasing hydrophobicity of the surface.

The temperature effects on hydrophobic hydration are demonstrated by Figures 4 and 5 (both Figures 4 and 5 are for a hydrophobic surface with $k_p = 2.1$ and the hydrogen bond energetic alteration ratio is taken to be 1). Figure 4 shows the temperature dependence of the Helmholtz free energy of hydration of a hydrophobic surface, while Figure 5 presents the temperature dependence of the energetic and entropic components of the hydration free energy.

In Figure 4, the solid and dashed curves correspond to WDA and LDA, respectively. The upper curves were obtained with the overall external potential in DFT formalism including both the pairwise and hydrogen-bond contributions (i.e., $U_{\text{ext}}(x) =$

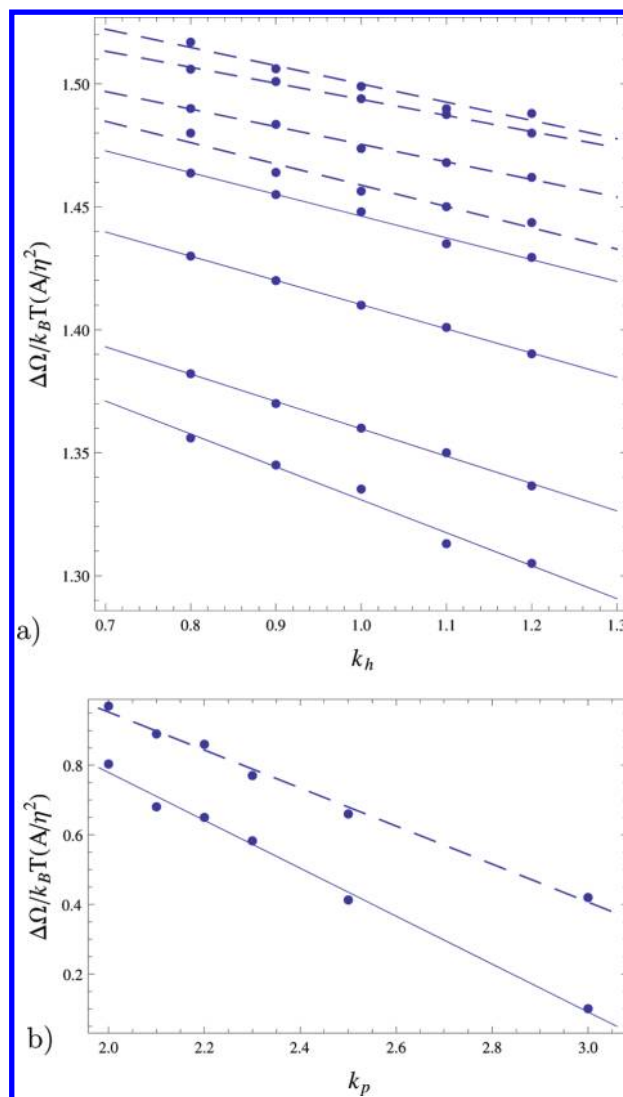


Figure 3. Grand canonical free energy of hydrophobic hydration, $\Delta\Omega$, expressed in units of $k_B T$ per A/η^2 (with A the area of the hydrophobic surface): (a) as a function of the bond energy alteration ratio k_h at a constant k_p . The solid lines represent WDA for surfaces of different degrees of hydrophobicity ($k_p = 2.0, 2.2, 2.3$, and 2.5 from top to bottom), whereas the dashed lines represent LDA for different surfaces ($k_p = 2.0, 2.1, 2.2$, and 2.3 from top to bottom); (b) as a function of k_p for $U_{\text{ext}}(x) = U_{\text{ext}}^{\text{pw}}(x)$. The dashed and solid curves are for LDA and WDA, respectively.

$U_{\text{ext}}^{\text{pw}}(x) + U_{\text{ext}}^{\text{hb}}(x)$), whereas the lower curves were obtained with **only** the pairwise component included in the external potential (i.e., $U_{\text{ext}}(x) = U_{\text{ext}}^{\text{pw}}(x)$). As expected, including a strong repulsive contribution $U_{\text{ext}}^{\text{hb}}(x)$ into $U_{\text{ext}}(x)$ significantly (by a factor of 2 or even more, depending on temperature T) increases the predictions of the combined PHB/DFT model (in both WDA and LDA) for the free energy of hydration of a large hydrophobic particle. In other words, the water hydrogen bonding constitutes an important factor in hydrophobic hydration of large-scale particles. Generalizing, in other words, the ability of the solvent to form hydrogen bonds makes the solvation process thermodynamically more *unfavorable* (i.e., significantly increasing the free energy of solvation).

Furthermore, in LDA the hydration free energy is predicted to decrease with increasing T (in the temperature range considered, from $T = 293$ K to $T = 333$ K) independent of whether

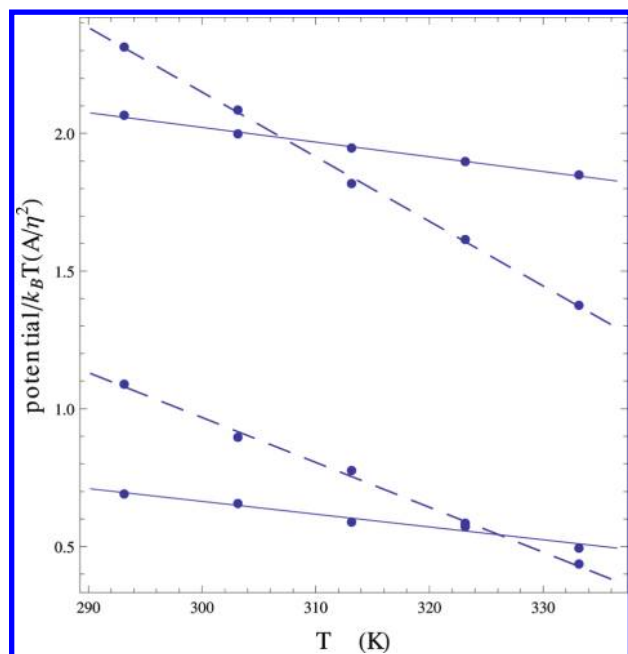


Figure 4. Temperature dependence of the Helmholtz free energy of hydration of a hydrophobic surface with $k_p = 2.1$ for $k_h = 1.0$. The solid and dashed curves correspond to WDA and LDA, respectively. Two upper curves are for $U_{\text{ext}}(x) = U_{\text{ext}}^{\text{pw}}(x) + U_{\text{ext}}^{\text{hb}}(x)$, whereas two lower curves are for $U_{\text{ext}}(x) = U_{\text{ext}}^{\text{pw}}(x)$.

$U_{\text{ext}}(x) = U_{\text{ext}}^{\text{pw}}(x)$ or $U_{\text{ext}}(x) = U_{\text{ext}}^{\text{pw}}(x) + U_{\text{ext}}^{\text{hb}}(x)$. On the other hand, in WDA the hydration free energy is predicted to decrease with increasing T for $U_{\text{ext}}(x) = U_{\text{ext}}^{\text{pw}}(x)$, while it is predicted to increase with increasing T for $U_{\text{ext}}(x) = U_{\text{ext}}^{\text{pw}}(x) + U_{\text{ext}}^{\text{hb}}(x)$ (although its ratio to $k_B T$ is still a decreasing function of T). The latter version of the combined PHB/DFT model (i.e., when WDA is used in DFT formalism and the hydrogen bond contribution is included in the external potential $U_{\text{ext}}(x)$), hereafter referred to as the combined PHB/DFT(WDA) model, is clearly most adequate and accurate. It is thus quite natural that its predictions are most consistent with expectations, according to the available experimental and simulational data on the hydration of small hydrophobes (less than 10 nm in linear sizes); the direct comparison with experiments is not possible because of the lack of data pertaining to the hydration of large-scale (macroscopic) hydrophobes.

Figure 5 presents the Helmholtz free energy of hydrophobic hydration, ΔF , and its energetic and entropic components, Φ_E and Φ_S , as functions of T (all of the potentials are expressed in units of $k_B T$ per dimensionless unit area as explained above). The solid curves represent ΔF itself, while the long-dashed and short-dashed curves are for Φ_E and Φ_S , respectively. The results obtained in WDA are shown in Figure 5a (for the external potential $U_{\text{ext}}(x) = U_{\text{ext}}^{\text{pw}}(x) + U_{\text{ext}}^{\text{hb}}(x)$) and Figure 5b (for the external potential $U_{\text{ext}}(x) = U_{\text{ext}}^{\text{pw}}(x)$), whereas the results by LDA are presented in Figure 5c (with $U_{\text{ext}}(x) = U_{\text{ext}}^{\text{pw}}(x) + U_{\text{ext}}^{\text{hb}}(x)$ in the upper panel and $U_{\text{ext}}(x) = U_{\text{ext}}^{\text{pw}}(x)$ in the lower panel).

As is clear from Figure 5, the combined PHB/DFT(WDA) model suggests that the hydration process is unfavorable both enthalpically and entropically; that is, both the enthalpic and the entropic contributions to the hydration free energy are positive (the former being much larger than the latter). The enthalpic contribution increases with increasing temperature, while the entropic one decreases and becomes virtually

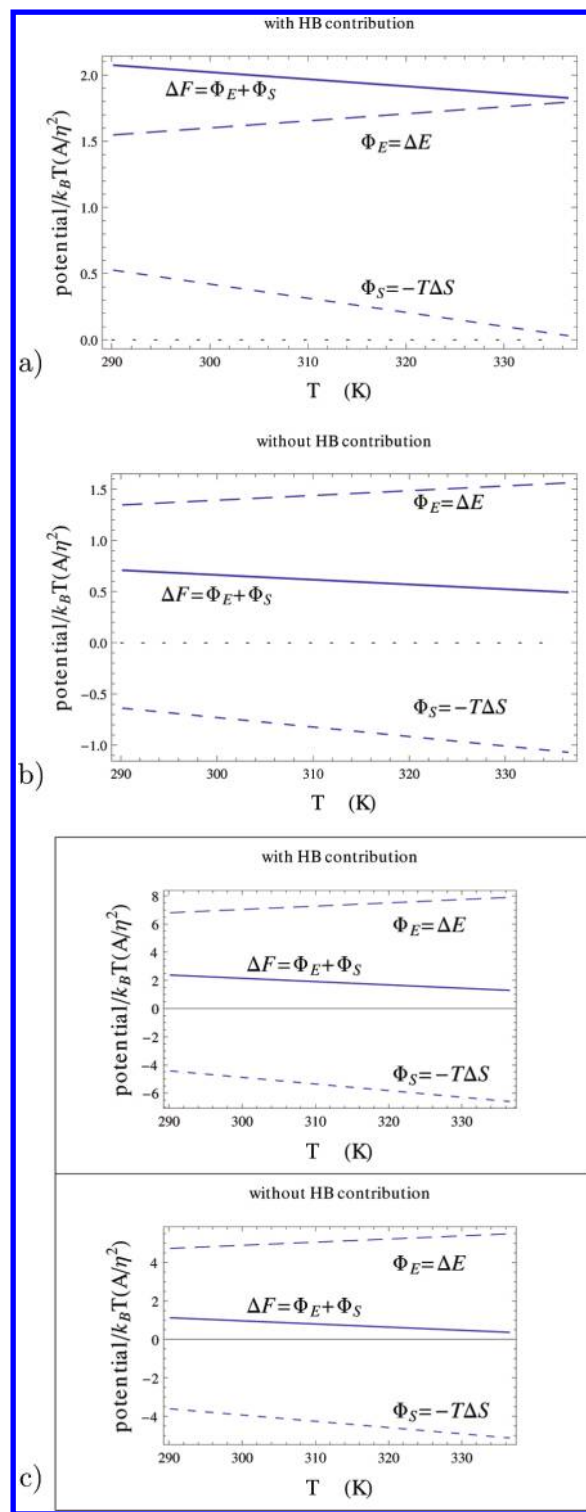


Figure 5. Helmholtz free energy of hydrophobic hydration, ΔF , and its energetic and entropic components, Φ_E and Φ_S , as functions of T for a hydrophobic surface with $k_p = 2.1$. a) The results of WDA with $U_{\text{ext}}(x) = U_{\text{ext}}^{\text{pw}}(x) + U_{\text{ext}}^{\text{hb}}(x)$ for $k_h = 1.0$; b) The results of WDA with $U_{\text{ext}}(x) = U_{\text{ext}}^{\text{pw}}(x)$; c) The results of LDA with $U_{\text{ext}}(x) = U_{\text{ext}}^{\text{pw}}(x) + U_{\text{ext}}^{\text{hb}}(x)$ for $k_h = 1.0$ (upper panel) and $U_{\text{ext}}(x) = U_{\text{ext}}^{\text{pw}}(x) + U_{\text{ext}}^{\text{hb}}(x)$ (lower panel). The solid curves represent ΔF itself, while the long-dashed and short-dashed curves are for Φ_E and Φ_S , respectively.

negligible at the higher end of the temperature range considered. Extrapolating this temperature dependence of the entropic contribution, one can suggest that at high enough

temperatures the hydration process may even become entropically favorable.

Currently, no experimental data on the thermodynamics of hydration of large hydrophobes are available in literature. However, the enthalpic impediment to the hydration of a large hydrophobe is quite expected^{12,13,27–29} (being due to the breaking of vicinal hydrogen bonds). On the other hand, while the entropic “insensitivity” (and may be “favorability”) of such hydration seems somewhat counterintuitive, there are indirect experimental and simulational indications of its physical soundness. For example, ref 50 reported an experimental observation that dissolving an argon molecule in hot liquid water leads to an increase in entropy (i.e., the hydration of an argon molecule is entropically favorable), although the transfer of the same molecule into cold liquid water causes a decrease in entropy (i.e., its hydration is entropically unfavorable). These experiments are supported by a theoretical model (the two-dimensional Mercedes-Benz model with one fitting parameter)⁵⁰ as well as by the molecular dynamics simulations of the SPC/E water model.⁵¹ The predictions of the combined PHB/DFT(WDA) model for the thermodynamics of the hydration of a flat hydrophobic surface are also qualitatively consistent with the MD simulation results^{40,52} for the hydrophobic attraction of large hydrophobic plates in a model liquid water (SPC/E in ref 40 and TIP4P/E in ref 52).

Furthermore, studying the length scale dependence of hydrophobic hydration (under various thermodynamic conditions) by means of MD simulations of SPC/E water model, it was demonstrated²³ that the hydration thermodynamics changes its character from “entropy dominated” to “enthalpy dominated” near the crossover region as the length scale of a hydrophobe increases. At $T = 300$ K and a pressure of -1000 atm, the crossover region was found to be around $R = 3$ nm (R being the radius of a spherical hydrophobe). As reported,²³ the hydration is predominantly entropic ($\Phi_S > \Phi_E > 0$), for solutes of radii smaller than 3 nm, whereas it is predominantly enthalpic ($\Phi_E > \Phi_S > 0$) for solutes of radii larger than 3 nm. As the radius of the solute increases, the enthalpic contribution Φ_E increases, whereas the entropic contribution Φ_S decreases and is expected to become negative “for sufficiently large solutes” (see ref 23). Qualitatively, this can be interpreted as the result of breaking the tetrahedrally ordered structure of water–water hydrogen bond network by the foreign hydrophobic particle; breaking the ordered structure of the hydrogen bond network is equivalent to somewhat increasing the disorder in the system which could lead to an increase in its entropy.

It should be noted that, knowing Φ_E as a function of T , one can find the change of the isochoric specific heat capacity upon hydration as $\Delta C_V = \partial \Phi_E / \partial T$. Let us define the dimensionless quantity $\Delta \tilde{C}_V \equiv \Delta C_V / (k_B A_{ij}^2)$ which represents ΔC_V expressed in units of k_B per dimensionless “unit area”. For the model system considered, the combined PHB/DFT(WDA) model predicts $\Delta \tilde{C}_V$ to be about 3.2 at $T = 300.15$ K. This value is consistent with the experimental data on ΔC_V for the hydration of propane and *n*-butane at the same temperature, as compiled in ref 19. Indeed, considering the *n*-butane molecule as a hydrophobic cylinder of length 8.24 Å and diameter 4.15 Å, one can obtain $\Delta \tilde{C}_V^{\text{but}} \approx 3.0$; modeling the propane molecule as a cylinder of length 6.95 and diameter 4.15 Å, one has $\Delta \tilde{C}_V^{\text{prop}} \approx 3.5$. Note that the agreement between the combined PHB/DFT(WDA) model and experimental data is better for a larger hydrophobic molecule (*n*-butane), as expected.

6. CONCLUDING REMARKS

To clarify some aspects of the effect of water–water hydrogen bonding on the thermodynamics of hydrophobic hydration, we have proposed a combination of our previously developed probabilistic approach to water–water hydrogen bonding with the classical DFT. The latter allows one to accurately determine the distribution of water molecules in the vicinity of a hydrophobic particle and calculate the thermodynamic quantities of hydrophobic hydration as well as their temperature dependence. The former allows one to implement the effect of the hydrogen-bonding ability of water molecules on their interaction with the hydrophobic surface into the DFT formalism.

The hydrogen bond network of water molecules affects their interaction with the hydrophobic surface because the number and energy of hydrogen bonds that a water molecule forms in the surface differ from their bulk values. Such an alteration gives rise to a short-range hydrogen bond contribution to the external potential field whereto a water molecule is subjected in that vicinity. This contribution is a dominant component of the interactions of a water molecule with the surface at distances between one and two hydrogen bond lengths. As we previously showed,³⁴ it plays a crucial role in the formation of a thin depletion layer (of thickness of a molecular diameter and of very low density, in agreement with previous suggestions^{12,13}) between liquid water and hydrophobic surface.

The combined PHB/DFT approach to hydrophobic hydration predicts that the free energy of hydration of a model hydrophobic surface in a model liquid water slightly increases with increasing temperature in the range from 293 to 333 K (so that its ratio to $k_B T$ decreases). The hydration process is unfavorable both enthalpically and entropically, with the latter effect decreasing with temperature and becoming negligible at the higher end of the temperature range considered. This corroborates the counterintuitive experimental and simulational observation that under some thermodynamic conditions the hydrophobic hydration may become slightly favorable entropically. As a possible explanation thereof, one could conjecture that the destruction of the tetrahedrally ordered structure of water hydrogen bond network by a hydrophobic particle may result in an increased disorder in the system which leads to an increase in its entropy.

AUTHOR INFORMATION

Corresponding Author

*E-mail: idjikaev@buffalo.edu.

Notes

The authors declare no competing financial interest.

†E-mail: feaeliru@buffalo.edu.

REFERENCES

- (1) Pimental, C. G.; McCellan, A. L. *The Hydrogen Bond*; W. H. Freeman: San Francisco, CA, 1960.
- (2) Schuster, P.; Zindel, G.; Sandorfy, C., Eds. *The Hydrogen Bond: Recent Developments in Theory and Experiments*; North Holland: Amsterdam, 1976.
- (3) (a) Chaplin, M. F. In *Water of Life: The unique properties of H₂O*; Lynden-Bell, R. M., Morris, S. C., Barrow, J. D., Finney, J. L., Harper, C., Eds; CRC Press: Boca Raton, FL, 2010; p 69. (b) Chaplin, M. F. *Water Structure and Science*, (e-Book, <http://www.lsbu.ac.uk/water/index.html>).
- (4) Sharp, K. A. *Curr. Opin. Struct. Biol.* **1991**, *1*, 171.
- (5) Soda, K. *Adv. Biophys.* **1993**, *29*, 1.

- (6) Paulaitis, M. E.; Garde, S.; Ashbaugh, H. S. *Curr. Opin. Colloid Interface Sci.* **1996**, *1*, 376.
- (7) Blokzijl, W.; Engberts, J. B. F. N. *Angew. Chem., Int. Ed. Engl.* **1993**, *32*, 1545–1579.
- (8) Anfinsen, C. B. *Science* **1973**, *181*, 223–230.
- (9) Ghelis, C.; Yan, J. *Protein Folding*; Academic Press: New York, 1982.
- (10) Kauzmann, W. *Adv. Protein Chem.* **1959**, *14*, 1–63.
- (11) Privalov, P. L. *Crit. Rev. Biochem. Mol. Biol.* **1990**, *25*, 281–305.
- (12) Ball, P. *Chem. Rev.* **2008**, *108*, 74–108.
- (13) Berne, B. J.; Weeks, J. D.; Zhou, R. *Annu. Rev. Phys. Chem.* **2009**, *60*, 85–103.
- (14) Frank, H.; Evans, M. J. *Chem. Phys.* **1945**, *13*, 507–532.
- (15) Stillinger, F. H. *J. Solution Chem.* **1973**, *2*, 141–158.
- (16) Pratt, L. R.; Chandler, D. *J. Chem. Phys.* **1977**, *67*, 3683–3704.
- (17) Müller, N. *Acc. Chem. Res.* **1990**, *23*, 23–28.
- (18) Lee, B.; Graziano, G. J. *Am. Chem. Soc.* **1996**, *118*, 5163–5168.
- (19) Widom, B.; Bhimlaparam, P.; Koga, K. *Phys. Chem. Chem. Phys.* **2003**, *5*, 3085–3093.
- (20) Pratt, L. R. *Annu. Rev. Phys. Chem.* **2002**, *53*, 409–436.
- (21) Lum, K.; Chandler, D.; Weeks, J. D. *J. Phys. Chem. B* **1999**, *103*, 4570–4577.
- (22) Southall, N. T.; Dill, K. A. *J. Phys. Chem. B* **2000**, *104*, 1326–1331.
- (23) Rajamani, S.; Truskett, T. M.; Garde, S. *Proc. Natl. Acad. Sci. U.S.A.* **2005**, *102*, 9475–9480.
- (24) Chandler, D. *Nature* **2005**, *437*, 640–647.
- (25) Pangali, C.; Rao, M.; Berne, B. J. *J. Chem. Phys.* **1979**, *71*, 2982–2990.
- (26) Watanabe, K.; Andersen, H. C. *J. Phys. Chem.* **1986**, *90*, 795–802.
- (27) Lee, C. Y.; McCammon, J. A.; Rossky, P. J. *J. Chem. Phys.* **1984**, *80*, 4448–4455.
- (28) Choudhury, N.; Pettitt, B. M. *Mol. Simul.* **2005**, *31*, 457–463.
- (29) Choudhury, N.; Pettitt, B. M. *J. Am. Chem. Soc.* **2007**, *129*, 4847–4852.
- (30) Evans, R. *Adv. Phys.* **1979**, *28*, 143–200.
- (31) Evans, R. In *Fundamentals of Inhomogeneous Fluids*; Henderson, D., Ed.; Marcel Dekker: New York, 1992.
- (32) Sullivan, D. E. *Phys. Rev. B* **1979**, *20*, 3991–4000.
- (33) Tarazona, P.; Evans, R. *Mol. Phys.* **1983**, *48*, 799–831.
- (34) Ruckenstein, E.; Djikaev, Y. S. *J. Phys. Chem. Lett.* **2011**, *2*, 1382–1386.
- (35) Djikaev, Y. S.; Ruckenstein, E. *J. Chem. Phys.* **2010**, *133*, 194105.
- (36) Djikaev, Y. S.; Ruckenstein, E. *Curr. Opin. Colloid Interface Sci.* **2011**, *16*, 272–284.
- (37) Meng, E. C.; Kollman, P. A. *J. Phys. Chem.* **1996**, *110*, 11460–11470.
- (38) Silverstein, K. A. T.; Haymet, A. D. J.; Dill, K. A. *J. Chem. Phys.* **1999**, *111*, 8000–8009.
- (39) Djikaev, Y. S.; Ruckenstein, E. *J. Chem. Phys.* **2009**, *130*, 124713.
- (40) Zangi, R.; Berne, B. J. *J. Phys. Chem. B* **2008**, *112*, 8634–8644.
- (41) Tarazona, P. *Phys. Rev. A* **1985**, *31*, 2672–2679.
- (42) Curtin, W. A.; Ashcroft, N. W. *Phys. Rev. A* **1985**, *32*, 2909–2919.
- (43) Lee, D. J.; Telo da Gama, M. M.; Gubbins, K. E. *J. Chem. Phys.* **1986**, *85*, 490–499.
- (44) Hill, T. L. *Statistical Mechanics: Principles and Selected Applications*; Dover Publications, Inc.: New York, 1987.
- (45) Nakanishi, H.; Fisher, M. E. *Phys. Rev. Lett.* **1982**, *49*, 1565–1568.
- (46) Kollman, P. A.; Allen, L. C. *Chem. Rev.* **1972**, *72*, 283–303.
- (47) Carnahan, N. F.; Starling, K. E. *J. Chem. Phys.* **1969**, *51*, 635–636.
- (48) Weeks, J. D.; Chandler, D.; Anderson, H. C. *J. Chem. Phys.* **1971**, *54*, 5237–5247.
- (49) Patel, A. J.; Varilly, P.; Chandler, D. *J. Phys. Chem. B* **2010**, *114*, 1632–1637.
- (50) Xu, H.; Dill, K. A. *J. Chem. Phys.* **2005**, *109*, 23611–23617.
- (51) Guillot, B.; Guissani, Y. *J. Chem. Phys.* **1993**, *99*, 8075–8094.
- (52) Zangi, R. *J. Phys. Chem. B* **2011**, *115*, 2303–2311.